

Modeling the Development of Elastic Anisotropy as a Result of Plastic Flow for Glassy Polycarbonate

A. Goel, K. Strabala, M. Negahban, J.A. Turner

Department of Engineering Mechanics, University of Nebraska-Lincoln, Lincoln, Nebraska 68588-0526

The development of anisotropy as a result of plastic deformation below the glass-transition temperature is investigated and modeled for amorphous polycarbonate. Initially, isotropic polycarbonate was subjected to different extents of plastic flow in compression, and the development of its anisotropic wave speed moduli were studied using ultrasonic wave speed measurements. Longitudinal and shear wave speed measurements were performed both in the axial and transverse directions, with respect to the axis of compression. The moduli clearly indicated the development of a transversely elastic response as a result of the uniaxial compression. The measured moduli were used to model the elastic response of polycarbonate using a model for stress that depends both on the elastic and plastic parts of the deformation. POLYM. ENG. SCI., 49:1951–1959, 2009. © 2009 Society of Plastics Engineers

INTRODUCTION

It is well known that the elastic response of many isotropic solid polymers becomes anisotropic as a result of plastic strain [1–8]. This is clearly seen in Fig. 1, which shows the axial and transverse wave moduli as a function of plastic strain in tension for poly vinyl chloride (PVC), poly(methyl methacrylate) (PMMA), polystyrene (PS), and bisphenol A polycarbonate (PC). As indicated in the figure, for each polymer the axial and transverse wave moduli are initially identical indicating the response is isotropic, and then gradually become different as the polymer is subjected to different extents of plastic deformation. Typically, as shown in the figure, for uniaxial tension the axial modulus increases and the transverse modulus decreases with the increase of plastic strain. The extent of this difference depends on the polymer. For the polymers shown in Fig. 1, clearly PC is the most sensitive to plastic strain, developing very large differences in the moduli along the two directions, even at relatively small plastic strains. Also, it should be noted that this difference

is on the order of the plastic strain (i.e., ~60% difference in modulus for ~60% plastic strain in tension).

Even though a large difference can develop between the axial and transverse moduli as a result of plastic flow, as shown in Fig. 1, this fact is frequently ignored and not reflected in the models that are developed. Many models that are used to characterize the behavior of glassy polymers for large deformations are based on a modeling structure similar to that of plasticity. Examples of such models are the models described in [9–23], which describe the stress as a function of only the elastic deformation. Without a parameter to characterize the anisotropy that develops as a result of plastic flow, these models preserve the initial symmetry (in most cases isotropy) of the elastic response. This is true even after plastic flow. To remedy this, in the modeling of stress one needs to introduce a structure parameter, such as the extent of plastic deformation, in addition to the extent of elastic deformation.

In the current work, ultrasonic wave speed measurements are used to characterize the change in the elastic moduli of PC after compression to different extents of plastic strain. These are then used to make a model for the elastic response of PC, using a model for stress that depends on both the elastic and plastic deformation gradients. The resulting model is a finite deformation model that at the limit of zero elastic strain reproduces the correct anisotropic elastic moduli measured by the ultrasonic method.

EXPERIMENTAL MEASUREMENTS

All tests were performed on Lexan 9034. Samples were cut from 1.27 cm thick sheets and tested without any thermal conditioning.

The compression and shear wave moduli were calculated using the standard wave equations

$$E = \rho v_l^2, \quad (1)$$

$$G = \rho v_s^2, \quad (2)$$

where E is the longitudinal (compression/tension) wave modulus, G is the shear wave modulus, ρ is the density,

Correspondence to: Mehrdad Negahban; e-mail: mnegahban@unl.edu
Contract grant sponsor: U.S. Army Research Laboratory (ARL); contract grant number: W911NF-04-2-0011.
DOI 10.1002/pen.21429
Published online in Wiley InterScience (www.interscience.wiley.com).
© 2009 Society of Plastics Engineers

v_l is the wave speed for longitudinal waves, and v_s is the wave speed for shear waves. The density was measured through a standard method based on weighing the samples in air and water. The compression and shear wave speeds were evaluated by using a standard pulse-echo method for waves produced using ultrasonic transducers in the 1–5 MHz range [24]. Figure 2 shows a schematic of the wave speed measurement method, which is based on dividing the distance traveled by the travel time. The method is based on using the same ultrasonic transducer to both produce and measure the wave profile. Once the signal is recorded using an oscilloscope, the time between two consecutive echoes is measured, noting that the impedance mismatch between the PC and the transducer results in each echo being out of phase from the previous echo, and the distance traveled is calculated to be twice the thickness of the sample. Figure 2 shows a typical digitized signal, where one can see the initial pulse and its echoes. Note that the flat peaks on the initial pulse are due to saturation of the oscilloscope signal and not an actual flat peak in the signal. The initial pulse is not used, only the echoes are used since the interaction between the transducer and the surface creates an initially complex signal. For the system to work, the surfaces need to be parallel, flat, and polished. The accuracy of this method is normally in the percent range, depending on the thickness, the character of the surfaces, the signals, and the density measurement. The resulting errors were obtained by linear error analysis using the uncertainty in density, thickness, and time of flight. These errors compared well with those from a different study in which samples of known materials were evaluated ultrasonically to study the effect of surface quality and thickness.

The experiments were performed on samples from a series of initially compressed PC cylinders. The PC cylinders were plastically strained to ~10%, 20%, 30%, and 40% at a strain rate of 0.01 1/s, and then left unloaded

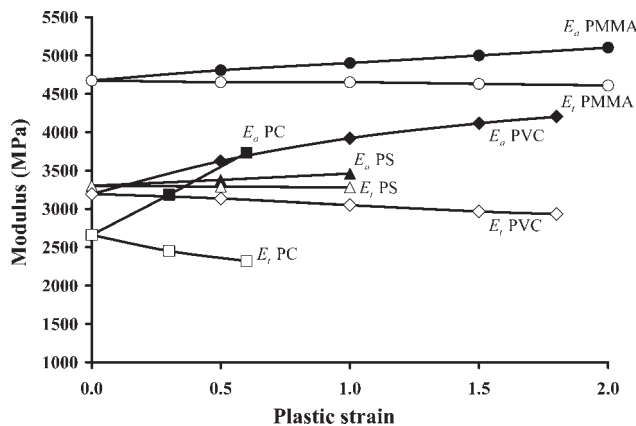


FIG. 1. Axial and transverse moduli reported as a function of the extent of plastic deformation in tension for PVC, PMMA, PS, and PC (from Ward [1]). As plastic strain increases, the axial longitudinal modulus E_a increases while the transverse longitudinal modulus E_t decreases.

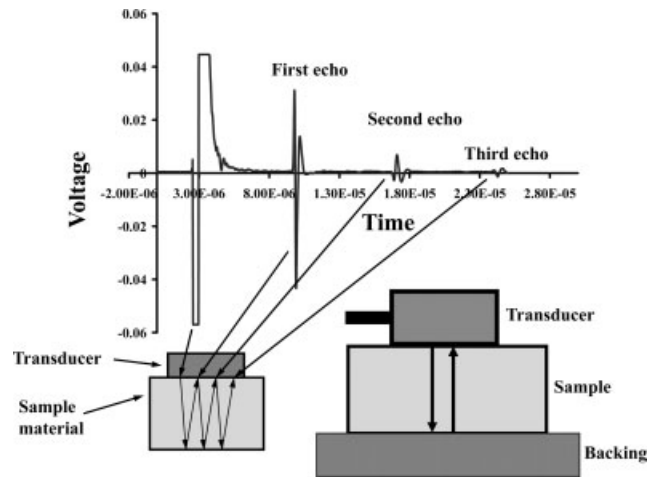


FIG. 2. Description of the pulse-echo method.

for at least 1 day before further testing. The recovery at this temperature after 1 day is minimal, and a study of the samples after 1 day showed no noticeable changes either in the permanent strain or wave measurements. The samples were then ultrasonically tested in the axial direction to calculate the associated longitudinal and shear wave speeds. From these wave speeds, the axial longitudinal wave modulus E_a and axial shear wave modulus G_a were calculated. The samples were then cut as shown in Fig. 3, and were ultrasonically tested to find the transverse longitudinal wave modulus E_t and transverse shear wave modulus G_t . The summary of the testing procedure is shown in Fig. 4. As shown in the figure, the axial shear wave modulus G_a was measured twice, once during axial wave speed measurements and again during transverse wave speed measurements (indicated as G'_a). The two measurements were identical indicating the sample was truly transversely isotropic.

Figures 5 and 6 show, respectively, the longitudinal and shear wave moduli that were measured. As can be seen in Fig. 5, the axial and transverse wave moduli are the same at zero plastic strain, indicating that the sample was initially isotropic. The difference between the axial and transverse moduli increases with increase in plastic strain, which indicates that the material develops more pronounced anisotropy with the increase of plastic strain. For the range of plastic strains considered, the axial wave modulus E_a decreases and the transverse wave modulus E_t increases with increase in the compressive plastic strain. The difference in these moduli is significant compared to the error in the measurement, as shown in the figure. Figure 6 shows the shear wave moduli along the different directions. As can be seen in the figure, the shear wave moduli G_a and G'_a are the same but different from G_t . The transverse shear wave modulus increases as the plastic strain in compression increases, while the axial shear wave modulus seems to remain constant.

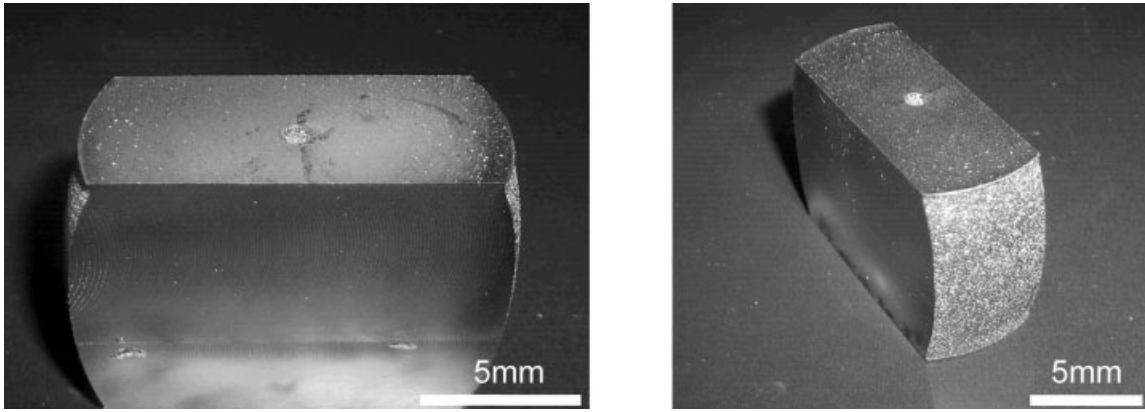


FIG. 3. Plastically compressed PC sample after cutting for transverse wave speed measurements.

MODELING CONSIDERATIONS

In developing a model to characterize the observed changes in the elastic moduli, we will consider an expression for the Cauchy stress \mathbf{T} that is a function of the elastic and plastic deformation gradients. This is done since traditionally used expressions [9–23], that only depend on the elastic deformation, do not allow modeling of a change in material symmetry in the elastic response. Specifically, we will construct a model based on a specific free energy ψ given by a function of the elastic deformation gradient \mathbf{F}^e , the plastic deformation gradient \mathbf{F}^p , and temperature θ . That is, we select a model of the form

$$\psi = \psi^+(\mathbf{F}^e, \mathbf{F}^p, \theta), \quad (3)$$

where the superscript “+” indicates the function used to model the variable, and we assume that the deformation gradient \mathbf{F} is decomposed through the multiplicative decomposition $\mathbf{F} = \mathbf{F}^e \mathbf{F}^p \mathbf{F}^\theta$, where \mathbf{F}^θ denotes the thermal deformation gradient. Imposing invariance to rigid body motions allows one to write the model for free energy as

$$\psi = \psi^+(\mathbf{U}^e, \mathbf{F}^p, \theta), \quad (4)$$

where \mathbf{U}^e is the right symmetric factor in the polar decomposition of \mathbf{F}^e . It also follows that the plastic deformation gradient in this equation can be shown to be indifferent to rigid body motions [25] if it is assumed that it can be calculated from the history of the deformation gradient. The initial symmetry of the material is characterized by a group of transformations \mathcal{G} containing members \mathbf{M} that reorganize the reference configuration [26, 27]. Each member \mathbf{M} in \mathcal{G} is a transformation of the reference configuration that leaves the reorganized neighborhood of the material point thermodynamically indistinguishable from the original neighborhood. That is, transformation of \mathbf{F} to $\mathbf{F}\mathbf{M}$, and the associated transformations of \mathbf{F}^e to $\mathbf{F}^e\mathbf{M}$ and \mathbf{F}^p to $\mathbf{M}^{-1}\mathbf{F}^p\mathbf{M}$, leave the value of free energy unchanged. For an orthogonal transformation \mathbf{M} , this requires that

$$\psi = \psi^+(\mathbf{U}^e, \mathbf{F}^p, \theta) = \psi^+(\mathbf{M}^T \mathbf{U}^e \mathbf{M}, \mathbf{M}^T \mathbf{F}^p \mathbf{M}, \theta). \quad (5)$$

For an initially isotropic material, with the reference configuration selected appropriately such that all the symmetry transformations are orthogonal [26], the constraint given by (5) must be satisfied for all orthogonal transformations. Since the decomposition of \mathbf{F}^p into its symmetric

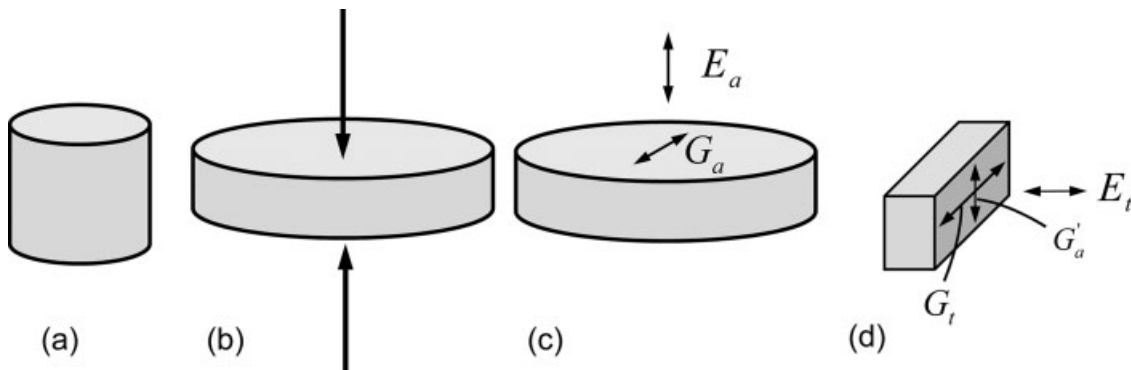


FIG. 4. Summary of testing: (a) original PC cylinder, (b) compressed PC cylinder, (c) ultrasonic testing in the axial direction, and (d) sample cut and ultrasonically tested in transverse direction.

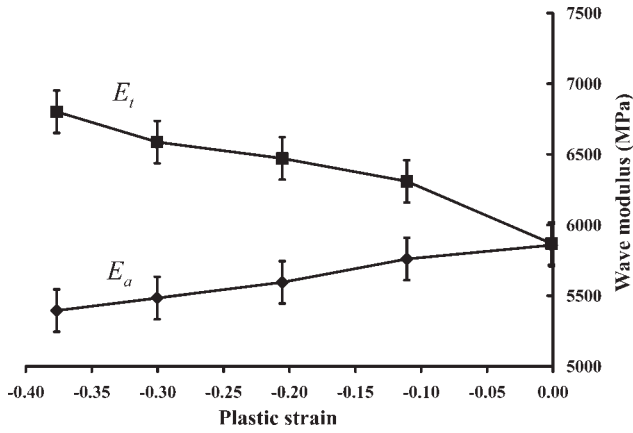


FIG. 5. Plot of axial and transverse longitudinal wave moduli measured at different plastic strains.

and skew symmetric parts is unique, one can use results given for the scalar isotropic invariants of two symmetric tensors [\mathbf{U}^e and $\mathbf{F}_{\text{sym}}^p = \frac{1}{2}(\mathbf{F}^p + \mathbf{F}^{pT})$] and one skew symmetric tensor [$\mathbf{F}_{\text{skew}}^p = \frac{1}{2}(\mathbf{F}^p - \mathbf{F}^{pT})$], as given by Spencer [28] and, more recently in reduced form, by Zheng [29] (also see [25]). Therefore, in general, one can construct a model for the specific free energy ψ in terms of the 21 isotropic invariants of \mathbf{U}^e , $\mathbf{F}_{\text{sym}}^p$, and $\mathbf{F}_{\text{skew}}^p$. Even though plausible, the number of invariants is too large to realistically be used in modeling the response, so we assume that the contribution of the plastic deformation gradient to the free energy is through the right Cauchy stretch tensor $\mathbf{C}^p = \mathbf{F}^{pT}\mathbf{F}^p$. This might be considered consistent with the assumption that the plastic deformation contributes to the free energy of a point through the strains it represents, not through its rigid body motion. We also use $\mathbf{C}^e = \mathbf{U}^e\mathbf{U}^e = \mathbf{U}^{e2}$ in place of \mathbf{U}^e , due to the convenience in the calculation of the former relative to the latter, and the fact that there is a one-to-one relation between them. As given by Spencer [28], there are 10 isotropic scalar invariants of \mathbf{C}^e and \mathbf{C}^p . These are given by

$$\begin{aligned} I_1 &= \text{tr}(\mathbf{C}^e), \quad I_2 = \text{tr}(\mathbf{C}^{e2}), \quad I_3 = \text{tr}(\mathbf{C}^{e3}), \quad I_4 = \text{tr}(\mathbf{C}^p), \\ I_5 &= \text{tr}(\mathbf{C}^{p2}), \quad I_6 = \text{tr}(\mathbf{C}^{p3}), \quad I_7 = \text{tr}(\mathbf{C}^e\mathbf{C}^p), \quad I_8 = \text{tr}(\mathbf{C}^{e2}\mathbf{C}^p), \\ I_9 &= \text{tr}(\mathbf{C}^e\mathbf{C}^{p2}), \quad \text{and} \quad I_{10} = \text{tr}(\mathbf{C}^{e2}\mathbf{C}^{p2}). \end{aligned} \quad (6)$$

Since the response of materials to volumetric deformations is normally vastly different from the response in shear, we construct a new, yet equivalent, set of invariants given by

$$\begin{aligned} I_1^* &= \frac{I_1}{J^{e3}}, \quad I_2^* = \frac{I_2}{I_1^2}, \quad I_3^* = J^e = \det(\mathbf{F}^e), \quad I_4^* = \frac{I_4}{J^{p3}}, \quad I_5^* = \frac{I_5}{I_4^2}, \\ I_6^* &= J^p = \det(\mathbf{F}^p), \quad I_7^* = I_7 - I_1 - I_4 + 3, \quad I_8^* = I_8 - I_2 - I_4 + 3, \\ I_9^* &= I_9 - I_1 - I_5 + 3, \quad \text{and} \quad I_{10}^* = I_{10} - I_2 - I_5 + 3, \end{aligned} \quad (7)$$

where the effect of volume changes are removed from I_1 , I_2 , I_4 , I_5 , and explicitly expressed in the form of the volume ratio in I_3^* and I_6^* .

Thus, we have an expression for specific free energy given by

$$\psi = \psi^+(I_1^*, \dots, I_{10}^*, \theta). \quad (8)$$

As has been shown in Negahban [25], as a result of the second law of thermodynamics, the Cauchy stress \mathbf{T} can be expressed as

$$\mathbf{T}^T = \rho \partial_{\mathbf{F}^e}(\psi) \mathbf{F}^{eT}, \quad (9)$$

where ρ is the current density. Considering the form of the specific free energy given in (8), the Cauchy stress can be expressed as

$$\mathbf{T}^T = \rho \sum_{i=1}^{10} \frac{\partial \psi}{\partial I_i^*} \partial_{\mathbf{F}^e}(I_i^*) \mathbf{F}^{eT}, \quad (10)$$

where from [30] we note that

$$\begin{aligned} \partial_{\mathbf{F}^e}(I_1^*) &= \frac{2}{J^{e2/3}} \left(\mathbf{F}^e - \frac{I_1}{3} \mathbf{F}^{e-T} \right), \quad \partial_{\mathbf{F}^e}(I_2^*) \\ &= \frac{4}{I_2^2} \mathbf{F}^e \left(\mathbf{C}^e - \frac{I_2}{I_1} \mathbf{I} \right), \quad \partial_{\mathbf{F}^e}(I_3^*) = J^e \mathbf{F}^{e-T}, \\ \partial_{\mathbf{F}^e}(I_4^*) &= \partial_{\mathbf{F}^e}(I_5^*) = \partial_{\mathbf{F}^e}(I_6^*) = 0, \quad \partial_{\mathbf{F}^e}(I_7^*) = 2\mathbf{F}^e(\mathbf{C}^p - \mathbf{I}), \\ \partial_{\mathbf{F}^e}(I_8^*) &= 2\mathbf{F}^e(\mathbf{C}^e\mathbf{C}^p + \mathbf{C}^p\mathbf{C}^e - 2\mathbf{C}^e), \\ \partial_{\mathbf{F}^e}(I_9^*) &= 2\mathbf{F}^e(\mathbf{C}^{p2} - \mathbf{I}), \\ \partial_{\mathbf{F}^e}(I_{10}^*) &= 2\mathbf{F}^e(\mathbf{C}^e\mathbf{C}^{p2} + \mathbf{C}^{p2}\mathbf{C}^e - 2\mathbf{C}^e). \end{aligned} \quad (11)$$

Substituting (11) into (10) results in an expression for the Cauchy stress as

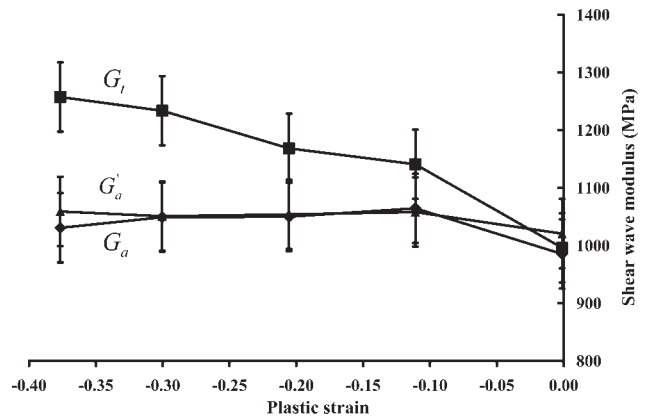


FIG. 6. Plot of axial and transverse shear wave moduli measured at different plastic strains.

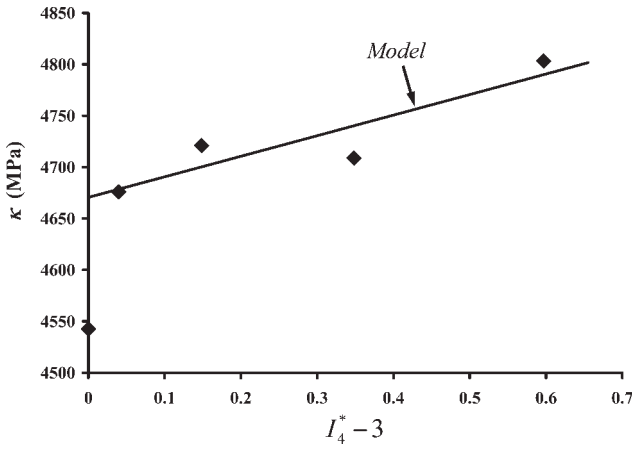


FIG. 7. Change of the isotropic bulk modulus with plastic deformation and associated fit by the model.

$$\mathbf{T} = \rho \left\{ \frac{2}{J^{e2/3}} \frac{\partial \psi}{\partial I_1^*} \left(\mathbf{B}^e - \frac{I_1}{3} \mathbf{I} \right) + \frac{4}{I_1^2} \frac{\partial \psi}{\partial I_2^*} \mathbf{B}^e \left(\mathbf{B}^e - \frac{I_2}{I_1} \mathbf{I} \right) + J^e \frac{\partial \psi}{\partial I_3^*} \mathbf{I} \right. \\ \left. + 2 \frac{\partial \psi}{\partial I_7^*} \mathbf{F}^e (\mathbf{C}^p - \mathbf{I}) \mathbf{F}^{eT} + 2 \frac{\partial \psi}{\partial I_8^*} \mathbf{F}^e (\mathbf{C}^e \mathbf{C}^p + \mathbf{C}^p \mathbf{C}^e - 2 \mathbf{C}^e) \mathbf{F}^{eT} \right. \\ \left. + 2 \frac{\partial \psi}{\partial I_9^*} \mathbf{F}^e (\mathbf{C}^{p2} - \mathbf{I}) \mathbf{F}^{eT} \right. \\ \left. + 2 \frac{\partial \psi}{\partial I_{10}^*} \mathbf{F}^e (\mathbf{C}^e \mathbf{C}^{p2} + \mathbf{C}^{p2} \mathbf{C}^e - 2 \mathbf{C}^e) \mathbf{F}^{eT} \right\}. \quad (12)$$

The stress should be zero for zero elastic strain, irrespective of the value of the plastic deformation gradient. Therefore, we should have $\mathbf{T} = \mathbf{0}$ for $\mathbf{F}^e = \mathbf{R}^e$, where \mathbf{R}^e can be any orthogonal tensor, and for all \mathbf{F}^p . This can be satisfied by setting

$$\begin{aligned} \frac{\partial \psi}{\partial I_3^*} &= 0, \\ \frac{\partial \psi}{\partial I_7^*} + 2 \frac{\partial \psi}{\partial I_8^*} &= 0, \\ \frac{\partial \psi}{\partial I_9^*} + 2 \frac{\partial \psi}{\partial I_{10}^*} &= 0, \end{aligned} \quad (13)$$

for $\mathbf{F}^e = \mathbf{R}^e$. One method to satisfy these conditions is to simply assume the last two conditions are always true (even when the elastic strain is not zero) and to take functions for the free energy that have a derivative, with respect to the third invariant, that is zero for $\mathbf{F}^e = \mathbf{R}^e$. Under such a condition the expression for stress is given by

$$\mathbf{T} = \rho \left\{ \frac{2}{J^{e2/3}} \frac{\partial \psi}{\partial I_1^*} \left(\mathbf{B}^e - \frac{I_1}{3} \mathbf{I} \right) + \frac{4}{I_1^2} \frac{\partial \psi}{\partial I_2^*} \mathbf{B}^e \left(\mathbf{B}^e - \frac{I_2}{I_1} \mathbf{I} \right) + J^e \frac{\partial \psi}{\partial I_3^*} \mathbf{I} \right. \\ \left. + \frac{\partial \psi}{\partial I_7^*} \mathbf{F}^e [2(\mathbf{C}^e - \mathbf{I}) - (\mathbf{C}^e \mathbf{C}^p + \mathbf{C}^p \mathbf{C}^e - 2 \mathbf{C}^e)] \mathbf{F}^{eT} \right. \\ \left. + \frac{\partial \psi}{\partial I_9^*} \mathbf{F}^e [2(\mathbf{C}^{p2} - \mathbf{I}) - (\mathbf{C}^e \mathbf{C}^{p2} + \mathbf{C}^{p2} \mathbf{C}^e - 2 \mathbf{C}^e)] \mathbf{F}^{eT} \right\}. \quad (14)$$

Even with these simplifications, five material functions, $\frac{\partial \psi}{\partial I_1^*}$, $\frac{\partial \psi}{\partial I_2^*}$, $\frac{\partial \psi}{\partial I_3^*}$, $\frac{\partial \psi}{\partial I_7^*}$, and $\frac{\partial \psi}{\partial I_9^*}$, need to be evaluated at

each loading point. Since we only have four elastic moduli per plastic strain, the fitting of all five would be impossible with the current experimental results. In addition, when confining the response to uniaxial compression, it can be shown that the expressions to fit the material functions result in a linear system with a singular coefficient matrix (see the Appendix), so only three conditions can be satisfied. As a result, we chose to set the derivative of the free energy with respect to I_2^* and I_9^* equal to zero, and to fit the three remaining derivatives to the four moduli using a least square fit. For the remainder of this article, we will focus on the model for stress given by

$$\mathbf{T} = \rho_0 \frac{\partial \psi}{\partial I_1^*} \frac{2}{J^{e2/3}} \left(\mathbf{B}^e - \frac{I_1}{3} \mathbf{I} \right) + \rho_0 \frac{\partial \psi}{\partial I_3^*} J^e \mathbf{I} \\ + \rho_0 \frac{\partial \psi}{\partial I_7^*} \frac{1}{J} \mathbf{F}^e [2(\mathbf{C}^p - \mathbf{I}) - (\mathbf{C}^e \mathbf{C}^p + \mathbf{C}^p \mathbf{C}^e - 2 \mathbf{C}^e)] \mathbf{F}^{eT}. \quad (15)$$

FITTING THE MODEL TO THE RESULTS FROM COMPRESSION

To fit the experimental data, we need to evaluate the wave moduli from the model, and to impose on the model the conditions of plastic flow during compression. Once this is done, we can use the experimental data to find the values of the three derivatives of the specific free energy given in Eq. 15.

We take \mathbf{e}_i to denote an orthonormal base with \mathbf{e}_3 along the direction of compression. During uniaxial compression, the plastic deformation gradient is of the form

$$\mathbf{F}^p = \lambda^{p*} \mathbf{e}_1 \otimes \mathbf{e}_1 + \lambda^p \mathbf{e}_2 \otimes \mathbf{e}_2 + \lambda^p \mathbf{e}_3 \otimes \mathbf{e}_3, \quad (16)$$

where λ^p is the plastic stretch in the axial direction (\mathbf{e}_3) and λ^{p*} is the plastic stretch in the transverse direction. These are taken to be the measured stretches of the sample after plastic deformation.

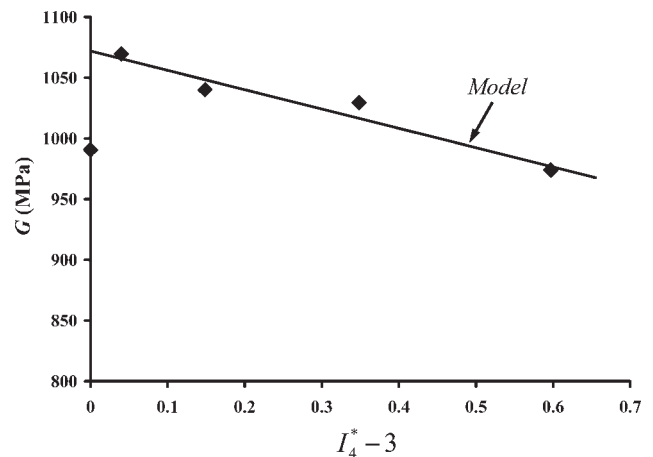


FIG. 8. Change of the isotropic shear modulus with plastic flow and the associated fit by the model.

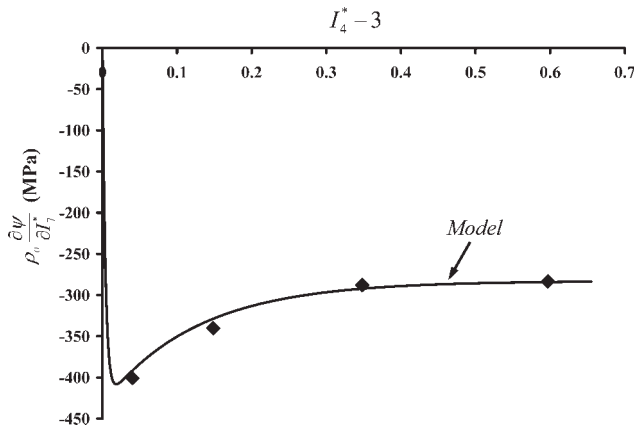


FIG. 9. Change of $\rho_0 \partial \psi / \partial I_7^*$ as a function of $I_4^* - 3$ and the associated fit by the model.

The components of the elastic deformation gradient and the stress in the base \mathbf{e}_i are taken, respectively, as \mathbf{F}_{ij}^c and \mathbf{T}_{ij} so that

$$\mathbf{F}^c = \mathbf{F}_{ij}^c \mathbf{e}_i \otimes \mathbf{e}_j, \quad (17)$$

$$\mathbf{T} = T_{ij} \mathbf{e}_i \otimes \mathbf{e}_j. \quad (18)$$

The wave moduli considered in the experiments can be evaluated from these components through the relations

$$\begin{aligned} E_a &= \left. \frac{\partial T_{33}}{\partial F_{33}^c} \right|_{\mathbf{F}^c = \mathbf{I}}, & E_t &= \left. \frac{\partial T_{11}}{\partial F_{11}^c} \right|_{\mathbf{F}^c = \mathbf{I}}, & G_a &= G'_a \\ &= \left. \frac{\partial T_{13}}{\partial F_{13}^c} \right|_{\mathbf{F}^c = \mathbf{I}}, & G_t &= \left. \frac{\partial T_{12}}{\partial F_{12}^c} \right|_{\mathbf{F}^c = \mathbf{I}}. \end{aligned} \quad (19)$$

These moduli were evaluated for the model and fit to the four measured moduli through a least squares fit. The result of this fit is shown in Figs. 7–9. The parameters κ and G in the figures, which, respectively, become associated with the isotropic bulk modulus and shear modulus, are defined in terms of the derivatives of the specific free energy as

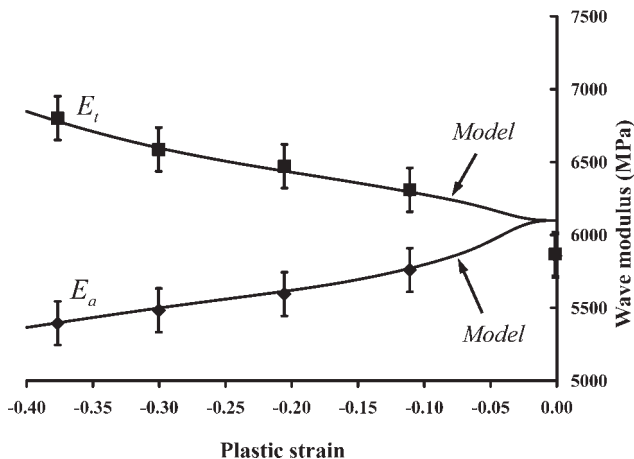


FIG. 10. Comparison of model results and experimentally measured wave moduli E_a and E_t shown for the given plastic strains.

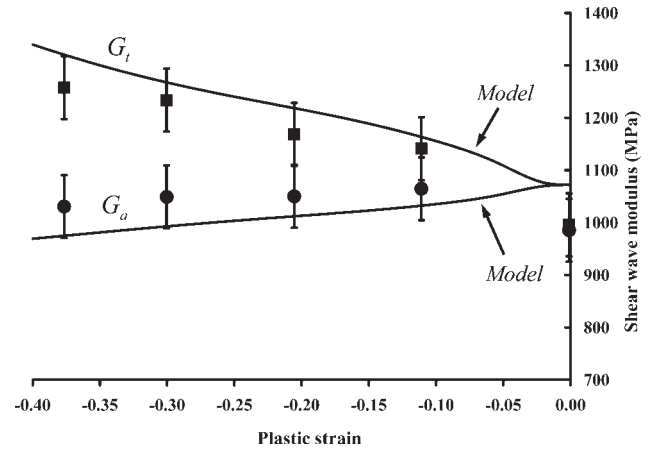


FIG. 11. Comparison of model results and experimentally measured wave moduli G_a and G_t shown for the given plastic strains.

$G = 2\rho_0 \partial \psi / \partial I_1^*$ and $k(1 - J^c) = \rho_0 \partial \psi / \partial I_3^*$. These curves were fit to the obtained variables using the functions

$$\kappa = 4670 + 200 \times (I_4^* - 3) \text{ MPa}, \quad (20)$$

$$G = 1072 - 159 \times (I_4^* - 3) \text{ MPa}, \quad (21)$$

$$\rho_0 \frac{\partial \psi}{\partial I_7^*} = -283 - 150 \times e^{-\frac{(I_4^* - 3)}{0.125}} + 433 \times e^{-\frac{(I_4^* - 3)}{0.004}} \text{ MPa}. \quad (22)$$

In constructing these models we have assumed that these are only a function of the plastic deformation gradient.

As shown in Figs. 10 and 11, which show the comparison of the experimental results for the wave moduli and those obtained from this fit, the fit accurately reproduces the observed wave moduli, with better results for the longitudinal waves as opposed to the shear waves.

In Figs. 12 and 13, we compare the model predictions with the results provided by Ward for PC after uniaxial tension [1], also shown in Fig. 1. As can be seen, the model trends follow those reported by Ward, but the magnitudes are different. This might be attributed to the fact that the current results were for wave moduli measured

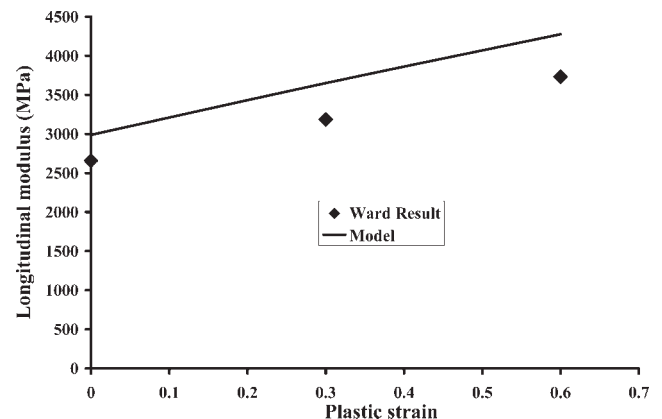


FIG. 12. Comparison between model predictions and results presented by Ward [1] for longitudinal modulus after extension.

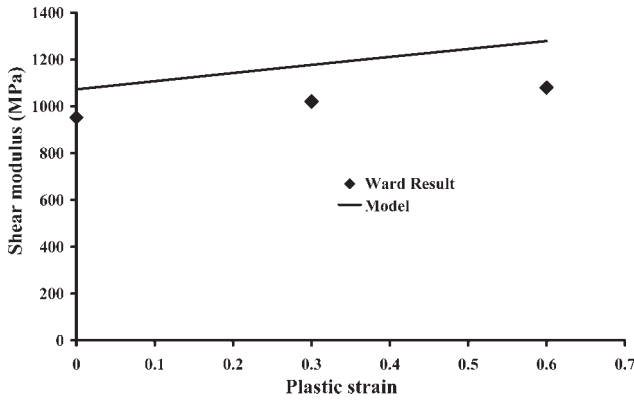


FIG. 13. Comparison between model predictions and results presented by Ward [1] for shear modulus after extension.

using a 1 MHz transducer as opposed to the results reported by Ward that were measured using frequencies in the range of 100–400 Hz.

SUMMARY AND CONCLUSION

This article focuses on measuring and modeling the anisotropic elastic response observed in PC after plastic deformation. Uniaxial compression was used to prepare samples with different extents of plastic deformation, up to ~40% compression (a logarithmic strain of approximately -0.5). Ultrasonic wave speed measurements were used to obtain the longitudinal and shear wave moduli both along the axis of compression and perpendicular to this axis. The transverse wave moduli, both longitudinal and shear, increased with plastic compression, while in the axial direction the longitudinal wave modulus decreased and the shear wave modulus stayed constant.

The extent of the difference in the wave moduli between axial and transverse directions for PC is substantial, indicating that ignoring this could result in substantial error in the predictions of the resulting models. These differences were in the same order as the imposed plastic strains (i.e., ~20% difference in moduli for 40% plastic compressive strain).

To capture the observed development of the anisotropic elastic moduli, a model for the free energy based on the elastic and plastic deformation gradients was constructed. Since the PC used was initially isotropic, representations for this model were provided for an initially isotropic material. This model was then simplified and fit to the experimental data. The resulting fits were in good agreement with the experimentally observed moduli, and predicted similar trends to experimental results reported in tension by Ward [1].

APPENDIX

Calculation of Stress and Its Rate

In this Appendix, it will be shown that the resulting model produces four independent material constants at each plastic strain for a condition of zero elastic strain,

but that only, at most, three can be calculated in a uniaxial test. This will be done by deriving the expression for the tangent modulus at a state of zero load and then will show that the system for uniaxial compression results in a system for the four values that has a coefficient matrix for the constants that is singular. The result is general and can be studied for other testing conditions to see how many of the constants can be evaluated.

The expression for Cauchy stress given in Eq. 14 can also be written as

$$\begin{aligned} \mathbf{T} = \rho \left\{ \frac{2}{J^{e2/3}} \frac{\partial \psi}{\partial I_1^*} \left(\mathbf{B}^e - \frac{I_1}{3} \mathbf{I} \right) + \frac{4}{I_1^2} \frac{\partial \psi}{\partial I_2^*} \mathbf{F}^e \left(\mathbf{C}^e - \frac{I_2}{I_1} \mathbf{I} \right) \mathbf{F}^{eT} \right. \\ \left. + J^e \frac{\partial \psi}{\partial I_3^*} \mathbf{I} + \frac{\partial \psi}{\partial I_7^*} \mathbf{F}^e [2(\mathbf{C}^e - \mathbf{I}) - \mathbf{C}^p (\mathbf{C}^e - \mathbf{I}) - (\mathbf{C}^e - \mathbf{I}) \mathbf{C}^p] \mathbf{F}^{eT} \right. \\ \left. + \frac{\partial \psi}{\partial I_9^*} \mathbf{F}^e [2(\mathbf{C}^e - \mathbf{I}) - \mathbf{C}^{p2} (\mathbf{C}^e - \mathbf{I}) - (\mathbf{C}^e - \mathbf{I}) \mathbf{C}^{p2}] \mathbf{F}^{eT} \right\}. \end{aligned} \quad (\text{A1})$$

It should be noted that the terms in the curly brackets “{ }” add to zero at zero elastic deformation (i.e., $\mathbf{F}^e = \mathbf{I}$). This is also true for all the terms in the round brackets “()”. Taking the derivative of \mathbf{T} and evaluating it at $\mathbf{F}^e = \mathbf{I}$, assuming plastic deformation gradients are constant, and after eliminating terms that are multiplied by $\frac{\partial \psi}{\partial I_3^*}$, “{ },” and “()” we find

$$\begin{aligned} \dot{\mathbf{T}} \Big|_{\mathbf{F}^e = \mathbf{I}} = \rho \left\{ 2 \frac{\partial \psi}{\partial I_1^*} \left(\dot{\mathbf{B}}^e - \frac{\dot{I}_1}{3} \mathbf{I} \right) + \frac{4}{9} \frac{\partial \psi}{\partial I_2^*} \left(\dot{\mathbf{C}}^e - \frac{\dot{I}_2}{I_1} \mathbf{I} \right) + \frac{\dot{\partial \psi}}{\partial I_3^*} \right. \\ \left. + \frac{\partial \psi}{\partial I_7^*} [2\dot{\mathbf{C}}^e - \mathbf{C}^p \dot{\mathbf{C}}^e - \dot{\mathbf{C}}^e \mathbf{C}^p] \right. \\ \left. + \frac{\partial \psi}{\partial I_9^*} [2\dot{\mathbf{C}}^e - \mathbf{C}^{p2} \dot{\mathbf{C}}^e - \dot{\mathbf{C}}^e \mathbf{C}^{p2}] \right\} \Big|_{\mathbf{F}^e = \mathbf{I}}. \end{aligned} \quad (\text{A2})$$

We first note that

$$\begin{aligned} \left(\dot{\mathbf{B}}^e - \frac{\dot{I}_1}{3} \mathbf{I} \right) \Big|_{\mathbf{F}^e = \mathbf{I}} &= \left(\dot{\mathbf{C}}^e - \frac{\dot{I}_2}{I_1} \mathbf{I} \right) \Big|_{\mathbf{F}^e = \mathbf{I}} \\ &= \dot{\mathbf{F}}^e + \mathbf{F}^{eT} - \frac{2}{3} (\mathbf{I} : \dot{\mathbf{F}}^e) \mathbf{I}. \end{aligned} \quad (\text{A3})$$

This allows us to write the stress rate as

$$\begin{aligned} \dot{\mathbf{T}} \Big|_{\mathbf{F}^e = \mathbf{I}} = \rho \left\{ 2 \left(\frac{\partial \psi}{\partial I_1^*} + \frac{2}{9} \frac{\partial \psi}{\partial I_2^*} \right) \left[\dot{\mathbf{F}}^e + \dot{\mathbf{F}}^{eT} - \frac{2}{3} (\mathbf{I} : \dot{\mathbf{F}}^e) \mathbf{I} \right] + \frac{\dot{\partial \psi}}{\partial I_3^*} \right. \\ \left. + \frac{\partial \psi}{\partial I_7^*} [2\dot{\mathbf{C}}^e - \mathbf{C}^p \dot{\mathbf{C}}^e - \dot{\mathbf{C}}^e \mathbf{C}^p] \right. \\ \left. + \frac{\partial \psi}{\partial I_9^*} [2\dot{\mathbf{C}}^e - \mathbf{C}^{p2} \dot{\mathbf{C}}^e - \dot{\mathbf{C}}^e \mathbf{C}^{p2}] \right\} \Big|_{\mathbf{F}^e = \mathbf{I}}. \end{aligned} \quad (\text{A4})$$

This shows that the derivative of the free energy with respect to the invariants I_1^* and I_2^* always appear in the same combination. Therefore, measurements that use stress rate at $\mathbf{F}^e = \mathbf{I}$ can only be used to evaluate the

given combination of these derivatives. Next, let us consider the term

$$\begin{aligned} \frac{\partial \bar{\psi}}{\partial I_3^*} \Big|_{\mathbf{F}^e=\mathbf{I}} &= \frac{\partial^2 \psi}{\partial I_1^* \partial I_3^*} \dot{I}_i^* \Big|_{\mathbf{F}^e=\mathbf{I}} = \left\{ \frac{\partial}{\partial I_3^*} \left(\frac{\partial \psi}{\partial I_3^*} \right) \mathbf{I} : \dot{\mathbf{F}}^e \right. \\ &+ 2 \left[\frac{\partial}{\partial I_7^*} \left(\frac{\partial \psi}{\partial I_3^*} \right) + 2 \frac{\partial}{\partial I_8^*} \left(\frac{\partial \psi}{\partial I_8^*} \right) \right] (\mathbf{C}^p - \mathbf{I}) : \dot{\mathbf{F}}^e \\ &\left. + 2 \left[\frac{\partial}{\partial I_9^*} \left(\frac{\partial \psi}{\partial I_3^*} \right) + 2 \frac{\partial}{\partial I_{10}^*} \left(\frac{\partial \psi}{\partial I_3^*} \right) \right] (\mathbf{C}^{p2} - \mathbf{I}) : \dot{\mathbf{F}}^e \right\}_{\mathbf{F}^e=\mathbf{I}}. \end{aligned} \quad (A5)$$

We now note that if we change the order of the derivatives in the square brackets “[],” both become zero as a result of the general conditions imposed on the relation between the derivatives of the free energy. We, thus, conclude that the expression for the stress rate evaluated at zero elastic deformation is given by

$$\begin{aligned} \dot{\mathbf{T}} \Big|_{\mathbf{F}^e=\mathbf{I}} &= \rho \left\{ 2 \left(\frac{\partial \psi}{\partial I_1^*} + \frac{2}{9} \frac{\partial \psi}{\partial I_2^*} \right) [\dot{\mathbf{F}}^e + \dot{\mathbf{F}}^{eT} - \frac{2}{3} (\mathbf{I} : \dot{\mathbf{F}}^e) \mathbf{I}] \right. \\ &+ \frac{\partial}{\partial I_3^*} \left(\frac{\partial \psi}{\partial I_3^*} \right) (\mathbf{I} : \dot{\mathbf{F}}^e) \mathbf{I} + \frac{\partial \psi}{\partial I_7^*} [2\dot{\mathbf{C}}^e - \mathbf{C}^p \dot{\mathbf{C}}^e - \dot{\mathbf{C}}^e \mathbf{C}^p] \\ &\left. + \frac{\partial \psi}{\partial I_9^*} [2\dot{\mathbf{C}}^e - \mathbf{C}^{p2} \dot{\mathbf{C}}^e - \dot{\mathbf{C}}^e \mathbf{C}^{p2}] \right\}_{\mathbf{F}^e=\mathbf{I}}, \end{aligned} \quad (A6)$$

where we note that

$$\dot{\mathbf{C}}^e \Big|_{\mathbf{F}^e=\mathbf{I}} = \dot{\mathbf{F}}^e + \dot{\mathbf{F}}^{eT}. \quad (A7)$$

In component form this can be written as

$$\begin{aligned} \dot{T}_{ij} &= \rho \left\{ 2 \left(\frac{\partial \psi}{\partial I_1^*} + \frac{2}{9} \frac{\partial \psi}{\partial I_2^*} \right) \left[\dot{F}_{ij}^e + \dot{F}_{ji}^e - \frac{2}{3} \dot{F}_{kk}^e \delta_{ij} \right] + \frac{\partial}{\partial I_3^*} \left(\frac{\partial \psi}{\partial I_3^*} \right) \dot{F}_{kk}^e \delta_{ij} \right. \\ &+ \frac{\partial \psi}{\partial I_7^*} [2(\dot{F}_{ij}^e + \dot{F}_{ij}^e) - C_{ik}^p (\dot{F}_{kj}^e + \dot{F}_{jk}^e) - (\dot{F}_{ik}^e + \dot{F}_{ki}^e) C_{kj}^p] \\ &\left. + \frac{\partial \psi}{\partial I_9^*} [2(\dot{F}_{ij}^e + \dot{F}_{ji}^e) - C_{ik}^{p2} (\dot{F}_{kj}^e + \dot{F}_{jk}^e) - (\dot{F}_{ik}^e + \dot{F}_{ki}^e) C_{kj}^{p2}] \right\}_{\mathbf{F}^e=\mathbf{I}}. \end{aligned} \quad (A8)$$

From this we can calculate the tangent modulus at zero elastic strain as

$$\begin{aligned} E_{ijmn} &= \rho \left\{ 2 \left(\frac{\partial \psi}{\partial I_1^*} + \frac{2}{9} \frac{\partial \psi}{\partial I_2^*} \right) [\delta_{im} \delta_{jn} + \delta_{jm} \delta_{in} - \frac{2}{3} \delta_{mn} \delta_{ij}] \right. \\ &+ \frac{\partial}{\partial I_3^*} \left(\frac{\partial \psi}{\partial I_3^*} \right) \delta_{mn} \delta_{ij} + \frac{\partial \psi}{\partial I_7^*} [2(\delta_{im} \delta_{jn} + \delta_{jm} \delta_{in}) \\ &- C_{ik}^p (\delta_{km} \delta_{jn} + \delta_{jm} \delta_{kn}) - (\delta_{im} \delta_{kn} + \delta_{km} \delta_{in}) C_{kj}^p] \\ &+ \frac{\partial \psi}{\partial I_9^*} [2(\delta_{im} \delta_{jn} + \delta_{jm} \delta_{in}) - C_{ik}^{p2} (\delta_{km} \delta_{jn} + \delta_{jm} \delta_{kn}) \\ &\left. - (\delta_{im} \delta_{kn} + \delta_{km} \delta_{in}) C_{kj}^{p2}] \right\}_{\mathbf{F}^e=\mathbf{I}} \end{aligned}$$

$$\begin{aligned} E_{ijmn} &= \rho \left\{ 2 \left(\frac{\partial \psi}{\partial I_1^*} + \frac{2}{9} \frac{\partial \psi}{\partial I_2^*} \right) [\delta_{im} \delta_{jn} + \delta_{jm} \delta_{in} - \frac{2}{3} \delta_{mn} \delta_{ij}] \right. \\ &+ \frac{\partial}{\partial I_3^*} \left(\frac{\partial \psi}{\partial I_3^*} \right) \delta_{mn} \delta_{ij} + \frac{\partial \psi}{\partial I_7^*} [2(\delta_{im} \delta_{jn} + \delta_{jm} \delta_{in}) \\ &- (C_{im}^p \delta_{jn} + C_{in}^p \delta_{jm} + \delta_{im} C_{nj}^p + \delta_{in} C_{mj}^p)] \\ &+ \frac{\partial \psi}{\partial I_9^*} [2(\delta_{im} \delta_{jn} + \delta_{jm} \delta_{in}) \\ &\left. - (C_{im}^{p2} \delta_{jn} + C_{in}^{p2} \delta_{jm} + \delta_{im} C_{nj}^{p2} + \delta_{in} C_{mj}^{p2})] \right\}_{\mathbf{F}^e=\mathbf{I}}. \end{aligned} \quad (A9)$$

Reorganizing this yields

$$\begin{aligned} E_{ijmn} &= \rho \left\{ 2 \left(\frac{\partial \psi}{\partial I_1^*} + \frac{2}{9} \frac{\partial \psi}{\partial I_2^*} + \frac{\partial \psi}{\partial I_7^*} + \frac{\partial \psi}{\partial I_9^*} \right) (\delta_{im} \delta_{jn} + \delta_{jm} \delta_{in}) \right. \\ &+ \left[\frac{\partial}{\partial I_3^*} \left(\frac{\partial \psi}{\partial I_3^*} \right) - \frac{4}{3} \left(\frac{\partial \psi}{\partial I_1^*} + \frac{2}{9} \frac{\partial \psi}{\partial I_2^*} \right) \right] \delta_{mn} \delta_{ij} \\ &- \frac{\partial \psi}{\partial I_7^*} (C_{im}^p \delta_{jn} + C_{in}^p \delta_{jm} + \delta_{im} C_{nj}^p + \delta_{in} C_{mj}^p) \\ &\left. - \frac{\partial \psi}{\partial I_9^*} (C_{im}^{p2} \delta_{jn} + C_{in}^{p2} \delta_{jm} + \delta_{im} C_{nj}^{p2} + \delta_{in} C_{mj}^{p2}) \right\}_{\mathbf{F}^e=\mathbf{I}}. \end{aligned} \quad (A10)$$

Denoting by

$$\begin{aligned} A &= 2\rho \left(\frac{\partial \psi}{\partial I_1^*} + \frac{2}{9} \frac{\partial \psi}{\partial I_2^*} + \frac{\partial \psi}{\partial I_7^*} + \frac{\partial \psi}{\partial I_9^*} \right)_{\mathbf{F}^e=\mathbf{I}}, \\ B &= \rho \left[\frac{\partial}{\partial I_3^*} \left(\frac{\partial \psi}{\partial I_3^*} \right) - \frac{4}{3} \left(\frac{\partial \psi}{\partial I_1^*} + \frac{2}{9} \frac{\partial \psi}{\partial I_2^*} \right) \right]_{\mathbf{F}^e=\mathbf{I}}, \end{aligned} \quad (A11)$$

$$C = -\rho \frac{\partial \psi}{\partial I_7^*} \Big|_{\mathbf{F}^e=\mathbf{I}},$$

$$D = -\rho \frac{\partial \psi}{\partial I_9^*} \Big|_{\mathbf{F}^e=\mathbf{I}},$$

we note that

$$\begin{aligned} E_{ijmn} &= A(\delta_{im} \delta_{jn} + \delta_{jm} \delta_{in}) + B \delta_{mn} \delta_{ij} + C(C_{im}^p \delta_{jn} \\ &+ C_{in}^p \delta_{jm} + \delta_{im} C_{nj}^p + \delta_{in} C_{mj}^p) \\ &+ D(C_{im}^{p2} \delta_{jn} + C_{in}^{p2} \delta_{jm} + \delta_{im} C_{nj}^{p2} + \delta_{in} C_{mj}^{p2}). \end{aligned} \quad (A12)$$

It is noted that the equation for stress can be written as

$$\begin{aligned} \mathbf{T} &= 2A\boldsymbol{\varepsilon}^e + B \text{tr}(\boldsymbol{\varepsilon}^e) \mathbf{I} + 2C(\mathbf{C}^p \boldsymbol{\varepsilon}^e + \boldsymbol{\varepsilon}^e \mathbf{C}^p) \\ &+ 2D(\mathbf{C}^{p2} \boldsymbol{\varepsilon}^e + \boldsymbol{\varepsilon}^e \mathbf{C}^{p2}), \end{aligned} \quad (A13)$$

for $\boldsymbol{\varepsilon}^e$ being the elastic infinitesimal strain tensor given in terms of the elastic displacement gradient $\mathbf{H}^e = \mathbf{F}^e - \mathbf{I}$ by

$$\boldsymbol{\varepsilon}^e = \frac{1}{2} (\mathbf{H}^e + \mathbf{H}^{eT}). \quad (A14)$$

The four moduli that we have measured are

$$\begin{aligned}
 E_a = E_{3333} &= 2A + B + 4C_{33}^p C + 4C_{33}^{p2} D, \\
 E_t = E_{1111} &= 2A + B + 4C_{11}^p C + 4C_{11}^{p2} D, \\
 G_a = E_{1313} &= A + (C_{11}^p + C_{33}^p)C + (C_{11}^{p2} + C_{33}^{p2})D, \\
 G_t = E_{1212} &= A + (C_{11}^p + C_{22}^p)C + (C_{11}^{p2} + C_{22}^{p2})D.
 \end{aligned}
 \tag{A15}$$

This can be written in a matrix equation for the four unknowns as

$$\begin{bmatrix}
 2 & 1 & 4C_{33}^p & 4C_{33}^{p2} \\
 2 & 1 & 4C_{11}^p & 4C_{11}^{p2} \\
 1 & 0 & C_{11}^p + C_{33}^p & C_{11}^{p2} + C_{33}^{p2} \\
 1 & 0 & C_{11}^p + C_{22}^p & C_{11}^{p2} + C_{22}^{p2}
 \end{bmatrix}
 \begin{bmatrix}
 A \\
 B \\
 C \\
 D
 \end{bmatrix}
 =
 \begin{bmatrix}
 E_a \\
 E_t \\
 G_a \\
 G_t
 \end{bmatrix}.
 \tag{A16}$$

For uniaxial compression we have $C_{11}^p = C_{22}^p$ and $C_{11}^{p2} = C_{22}^{p2}$ so that we can write

$$\begin{bmatrix}
 2 & 1 & 4C_{33}^p & 4C_{33}^{p2} \\
 2 & 1 & 4C_{11}^p & 4C_{11}^{p2} \\
 1 & 0 & C_{11}^p + C_{33}^p & C_{11}^{p2} + C_{33}^{p2} \\
 1 & 0 & 2C_{11}^p & 2C_{11}^{p2}
 \end{bmatrix}
 \begin{bmatrix}
 A \\
 B \\
 C \\
 D
 \end{bmatrix}
 =
 \begin{bmatrix}
 E_a \\
 E_t \\
 G_a \\
 G_t
 \end{bmatrix}.
 \tag{A17}$$

By examination, it can be seen that the coefficient matrix for this system is singular. Therefore, the solution to the unknowns A , B , C , and D cannot be obtained from this expression for experiments in uniaxial compression.

REFERENCES

1. I.M. Ward, *Mechanical Properties of Solid Polymers*, Wiley, NY, 293 (1979).
2. V.J. Hennig, *Kolloidzeitschrift*, **200**, 46 (1964).
3. F.F. Rawson and J.G. Rider, *J. Phys. D*, **7**, 41 (1974).
4. H. Wright, C.S.N. Faraday, E.F.T. White, and L.R.G. Treloar, *J. Phys. D*, **4**, 2002 (1971).
5. M. Kashiwagi, M.J. Folkes, and I.M. Ward, *Polymer*, **12**, 697 (1971).
6. H.H. Kausch, *J. Appl. Phys.*, **38**, 4213 (1967).
7. H.H. Kausch, *Polymer Fracture*, Springer-Verlag, Berlin, 33 (1978).
8. R.E. Robertson and R.J. Buenker, *J. Polym. Sci.*, A2, **2**, 4889 (1964).
9. A.S. Argon, *Polymer Materials: Relationship Between Structure and Mechanical Behavior*, American Society for Materials, 411 (1975).
10. A.S. Argon and M.I. Bessonov, *Polym. Eng. Sci.*, **17**, 3 (1977).
11. A.S. Argon and M.I. Bessonov, *Philos. Mag.*, **35**, 917 (1977).
12. M.C. Boyce, D.M. Parks, and A.S. Argon, *Mech. Mater.*, **7**, 15 (1988).
13. M.C. Boyce, D.M. Parks, and A.S. Argon, *Int. J. Plast.*, **5**, 593 (1989).
14. M.C. Boyce and E.M. Arruda, *Polym. Eng. Sci.*, **30**, 1288 (1990).
15. E.M. Arruda and M.C. Boyce, *Int. J. Plast.*, **9**, 697 (1993).
16. E.M. Arruda and M.C. Boyce, ASME MD Volume: *Use of Plastics and Plastic Composites: Materials and Mechanical Issues*, **46**, 23 (1993).
17. E.M. Arruda and M.C. Boyce, *Int. J. Plast.*, **9**, 783 (1993).
18. M.C. Boyce, E.M. Arruda, and R. Jayachandran, *Polym. Eng. Sci.*, **34**, 716 (1994).
19. M.C. Boyce, E.M. Arruda, and R. Jayachandran, *Mech. Mater.*, **19**, 193 (1995).
20. O.A. Hasan, M.C. Boyce, X.S. Li, and S. Berko, *Polym. Eng. Sci.*, **35**, 331 (1995).
21. E.M. Arruda, M.C. Boyce, and R. Jayachandran, *Mech. Mater.*, **19**, 193 (1995).
22. E. Krempl and K. Ho, *Polym. Eng. Sci.*, **35**, 310 (1995).
23. E. Krempl and C.M. Bordonaro, *ASTM Special Technical Publication*, 118 (2000).
24. G.L. Workman, D. Kishoni, and P.O. Moore, Eds., *Non-destructive Testing Handbook*, Chapter 7, *Ultrasonic Testing*, ASNT, Columbus (2007).
25. M. Negahban, *Int. J. Plast.*, **11**, 679 (1995).
26. M. Negahban and A.S. Wineman, *Int. J. Plast.*, **8**, 519 (1992).
27. M. Negahban and A.S. Wineman, *Appl. Mech. Div. Publ.*, **158**, 19 (1993).
28. A.J.M. Spencer, "Theory of Invariants," in *Continuum Physics: Volume 1—Mathematics*, A.C. Eringen, Ed., Academic Press, New York (1971).
29. Q.-S. Zheng, *Int. J. Eng. Sci.*, **31**, 1399 (1993).
30. M. Negahban, A. Goel, and L. Zhang, *Acta Mech.*, DOI: 10.1007/s00707-009-0139-6.